Received April 5, 2021, accepted April 22, 2021, date of publication May 4, 2021, date of current version May 13, 2021.

Digital Object Identifier 10.1109/ACCESS.2021.3077365

Optimized Design for Cable-Driven Shoulder-Elbow Exoskeleton Robot

KE SHI, AIGUO SONG, (Senior Member, IEEE), AND HUIJUN LI
School of Instrument Science and Engineering, Southeast University, Nanjing 210096, China

Corresponding author: Aiguo Song (a.g.song@seu.edu.cn)

This work was supported in part by the National Key Research and Development Program of China under Grant 2017YFB1303201, and in part by the Key Research and Development Program of Jiangsu Province under Grant BE2018004-4.

ABSTRACT The cable-driven exoskeletons have the advantages of low inertia and simple structure, and they are widely applied for human augmentation and rehabilitation. However, they have limited workspace and tension efficiency because of the unidirectional nature of the cables. The limited performance affects the human-robot interaction and leads to potential danger. The workspace and tension efficiency can be optimized by conventional methods, which are adjusting the cable attachment points and increasing the actuators. But the workspace still cannot cover the human joint space of activities of daily living, and the efficiency is also not high. This paper analyzed the specific application for shoulder and elbow joints rehabilitation and proposed a dynamic adaptive structure. This design can increase the workspace and improve tension efficiency greatly. The dynamic compensation control strategy is designed for the optimized system. Besides, in order to reduce the effects of compliant elements (e.g., cables or Bowden cables) between the actuators and output, and to improve the force bandwidth, we designed the distributed active semi-active system composed of the geared DC motor and magnetorheological clutches, which has low output inertia. The related experiments are carried out based on several healthy subjects. The results verified that the exoskeleton with the dynamic adaptive structure has a large workspace covering the activities of daily living joint space, high tension efficiency, and high force bandwidth, which is beneficial for the safety and comfort of human-robot interaction during rehabilitation training.

INDEX TERMS Cable-driven robot, rehabilitation robot, human–robot interaction, mechanism design, distributed active semi-active systems.

I. INTRODUCTION

Robot-assist rehabilitation for post-stroke patients has been proven to promote the recovery of motor function [1]. In general, the exoskeletons have better flexibility and larger workspace than the end-effector robots, but their structures are more complicated generally, and it is more difficult for them to meet the requirements of the joint alignment at the joint without a fixed rotation center, like shoulder joint. Some researchers have adopted a more complex redundant mechanism to avoid the misalignment, but the simplicity of the structure and the stability of the system are still sacrificed. In addition, the conventional rigid exoskeletons usually have large inertia and size, which affect the performance and wearing comfort of the robots [2], [3].

Because of the lightweight, low inertia, simple structure, and no joint misalignment, the cable-driven robot can be applied for rehabilitation training. It should be noted that the cable-driven robots can be divided into cable-transmitted robots like [4], [5] and cable-driven robots like [6], [7], but only the cable-driven robots are discussed in this paper because the cable-transmitted robots have some similar features to the rigid exoskeleton, like that their joints all need to be aligned with the human joints. Cable-driven robots are not only applied in the field of rehabilitation training and human augmentation but also in the industrial field [8], [9]. This paper mainly analyzes and optimizes the robot for shoulder-elbow joint rehabilitation training. In fact, the shoulder joint is mainly discussed because the elbow joint is only one degree of freedom (DOF) and is easily implemented.

The cable can only be pulled in the direction of the cable, so it has a bad impact on the workspace and efficiency of the cable-driven robot. The cable-driven robot needs to meet the cable tension strategy, that is, for the given end resultant force/torque, each cable must generate and only generate a positive tension along the direction of the cable.

The associate editor coordinating the review of this manuscript and approving it for publication was Dingguo Zhang.

The end resultant force/torque can be considered to keep zero when calculating the feasible workspace or compensate for the gravity of the limb and exoskeleton. In consideration of practical use, the cable tension should be limited to a certain range to keep tension and avoid excessive tension. According to the related researches of the cable-driven robot, the n DOF robot requires at least $n + 1$ cables to drive [10], [11]. And the number of cables should not exceed $2n$. Because too many cables will cause unnecessary redundancy and will not increase performance significantly.

For shoulder-elbow rehabilitation robots, the shoulder joint is generally considered to have three DOFs, which are flexion/extension, abduction/adduction, and internal/external rotation. The complex movement of the glenohumeral joint is ignored here because for the cable-driven exoskeleton, although it is difficult to actively control this movement, passive adaptation of the center shift and elimination of joint misalignment are its inherent characteristics [12], [13]. Therefore, the cable-driven robot for shoulder joint rehabilitation is usually designed with four to six cables [6], [7], [14], [15]. Of course, there are some robots with only three or two cables, but it is difficult for them to complete the shoulder joint movement of three DOFs [16], [17].

As mentioned above, the workspace of cable-driven robots is small due to the unidirectional nature of the cables. For the existing cable-driven shoulder exoskeletons like [6], [7], [18], even if the structure is optimized, their workspace still cannot cover the human activities of daily living (ADLs) space, and there is a large gap. As for [16] and [17], the workspace is much smaller than the human joint space, and they cannot even be completely controlled based on cable tension strategy. On the issue about workspace, it is different for the rigid and cable-driven exoskeletons. For the conventional rigid exoskeleton, the feasible workspace is usually large, and space will be limited during actual training to avoid injury from exceeding the range of the human joint space. But for the cable-driven exoskeleton, the workspace is usually small, and the robot will be uncontrollable when it is out of the feasible workspace. This disadvantage causes potential danger, especially for patients with weak motor capacity, so the trajectory out of the feasible workspace must be avoided. For example, due to the limitation of the workspace, the cable attachment points (CAPs) of CAREX/CAREX-7 need to be adjusted manually according to the reference trajectory to meet the requirements and avoid uncontrollability, but it increases the complexity of operation [6], [18]. The actual workspace of the robot can also be limited far from the boundary of the feasible workspace, and the limb is confined within this small range through specific control algorithms, but it also limits the effect of rehabilitation training.

As shown in Figure 1, on the other hand, because the tension can only be generated in the direction of the cable, when the required joint torque is provided, a force along the limb axis is generated, which is called parasitic force. Although the human joint can withstand large pressures, excessive

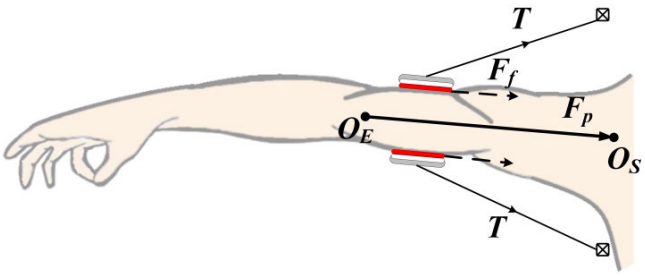

FIGURE 1. The schematic diagram of friction and parasitic force. The cables are simplified into two, the gray and white areas are the section of the upper arm module, and the red area is the contact surfaces between the exoskeleton and skin. OE and OS are the elbow and shoulder joint centers, respectively. T, F_f, and F_p represent the cable tension, friction, and parasitic force, respectively.

parasitic forces may cause relative sliding between the arms and exoskeleton. In the meantime, the friction between the exoskeletons and the limb will cause damage to the skin. The cable tension efficiency can be defined as the magnitude of the torque acting on the shoulder joint generated by the same tension condition. The greater the torque, the higher the tension efficiency. At the same time, the smaller the parasitic force acting on the joint, the higher the comfort of training. On the contrary, under the same tension condition, the torque acting on the joint smaller, the lower the efficiency, and the greater the parasitic force. In fact, the workspace and the tension efficiency are related, and the small workspace also means that the low average cable tension efficiency throughout the space, which is not beneficial for rehabilitation training.

By optimizing the distribution of the CAPs or increasing the number of cables, the workspace and tension efficiency can be improved to a certain extent, but the improvement is very limited. To address the above issues, based on optimizing the distribution of the CAPs, this paper proposed the dynamic adaptive structure (DAS) to improve the performance without excessively increasing the complexity of the structure. The distribution of the CAPs can be adjusted dynamically under the control of the DAS, so the workspace and tension efficiency of the robot is improved greatly.

The previous research has confirmed the importance of force bandwidth to the rehabilitation robot. However, because the application of traditional electromechanical actuators introduces high intrinsic inertia, the compliant element (cables or Bowden cables) between the actuators and the output component of the robot lowers the natural frequency of the system, thus limiting its dynamic performance [19]. In order to improve the force bandwidth performance and reduce the influence of the elastic elements of the cable-driven exoskeleton system, the distributed active semi-active (DASA) drive system based on the magnetorheological (MR) clutches is adopted. The magnetorheological clutch has low inertia and large output torque. In our previous work, the MR-DASA system has been tested on cable-driven wrist robotic, and its cable tension control performance was improved [20]. The DASA system can distribute the tension

to each cable from the force/torque source, which fits the antagonism characteristic of the parallel cable-driven system. In the meantime, due to the inherent damping of the MR clutches in the DASA system, the cable can be kept tension without any other special design.

In summary, compared with existing cable-driven rehabilitation exoskeletons, there are two main contributions of the proposed exoskeleton:

1) It has the largest workspace and highest cable tension efficiency, which is achieved by the development of the DAS. It eliminates the potential danger arising from the small workspace and lowers the parasitic force that is not beneficial for comfort and safety.

2) The MR-DASA system is proposed to improve the insufficient cable tension control performance caused by the large inertia of the traditional actuators. It improves the human-robot interaction performance and training safety.

The rest of this paper is organized as follow: Section II introduces the optimization method and the design of the DAS and MR-DASA drive system; Section III analyzes the workspace and cable tension efficiency of the optimized system; Section IV proposes the control algorithm applied to this system and Section V conducts the experiments based on healthy people to verify the effectiveness of the structure, drive system and algorithm; Section VI discusses and concludes this paper.

II. OPTIMIZATION METHOD AND SYSTEM DESIGN

A. THE OPTIMIZATION OF THE EXOSKELETON MECHANICAL DESIGN

It should be noted that the shoulder joint has a very large range of motion. If the robot structure is optimized with the full joint space as the target space, it is very difficult to realize the goal. Even the target space is realized, the average tension efficiency will be extremely low in ADLs space. This trade-off is meaningless, especially for rehabilitation training. Therefore, the optimization goal in this paper is to enable the robot workspace to cover the ADLs space to meet the daily rehabilitation training needs, as shown in Table 1.

TABLE 1. Rom of arm and robot joints.

Joint	Arm	Robot
(S)Flexion+/extesion-,q_1	[-25°,80°]	[-25°,80°]
(S)adduction+/abduction-, q_2	[-120°,25°]	[-120°,25°]
(S)Internal+/external-rotation,q_3	[-90°,90°]	[-90°,90°]
(E)Flexion+/extesion-,q_4	[0°,150°]	[0°,110°]

It has been explained in Section I that the cable-driven exoskeleton usually has a small workspace due to the inherent nature of the cable, only providing pull in its direction. As shown in Figure 2, to address the specific issue of the shoulder joint, the arm and exoskeleton are simplified. The shoulder joint is equivalent to a spherical joint, and its center is located at OS. Considering actual wearing, the radius of the shoulder bracket cannot be infinitely large, the radius of the upper arm module cannot be infinitely small, and the length of the arm is generally set as a constant.

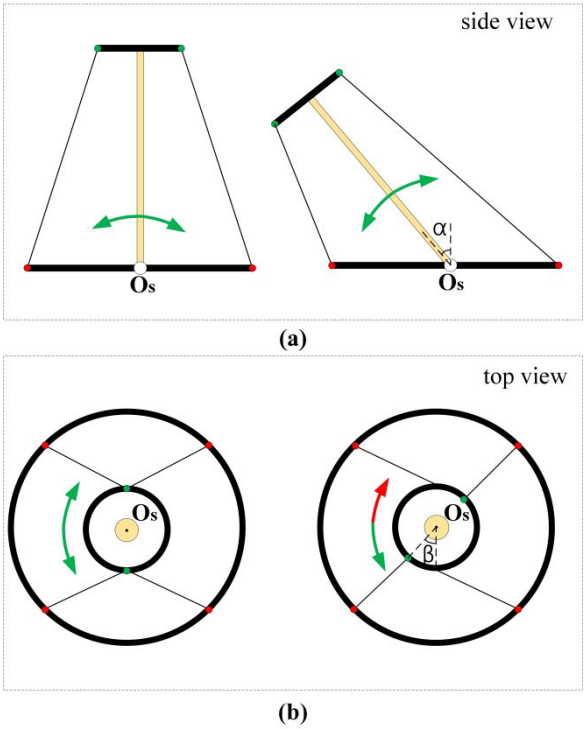

FIGURE 2. The short black rod and the small black circle represent the upper arm module, OS is the shoulder joint center, the long black rod and the large black circle represent the shoulder bracket, the yellow rod and circle represent the upper arm, and the thin black line represents the cables. The red dots are the CAPs of the shoulder bracket, and the green dots are the CAPs of the upper arm module.

As shown in Figure 2 (a), for a cable-driven robot, it is not very difficult to achieve the flexion/extension and abduction/adduction movement in the ADLs range. Even if the distribution of the CAPs is not deliberately optimized, the movement of these two DOFs can be completed easily. At the same time, the singularities never appear at these two DOFs. Nevertheless, in the internal/external rotation movement, with the continuous change of the cable configuration, the tension efficiency in this direction is getting lower and lower, and it will soon reach the singularity. Considering that the cable needs to be prevented from interfering with the limb and other cables during the movement, it is difficult to set the distribution of the CAPs to meet the needs of workspace for the internal/external rotation DOF in the current design.

In other words, if the workspace of the flexion/extension and abduction/adduction DOFs is optimized together with the internal/external rotation DOF, the workspace and efficiency of these two DOFs will be greatly reduced, and the overall performance will be affected. Therefore, the core problem is defined as how to eliminate the singularity of the internal/external rotation DOF and improve its effective range of motion, thereby improving the overall workspace and efficiency of three DOFs.

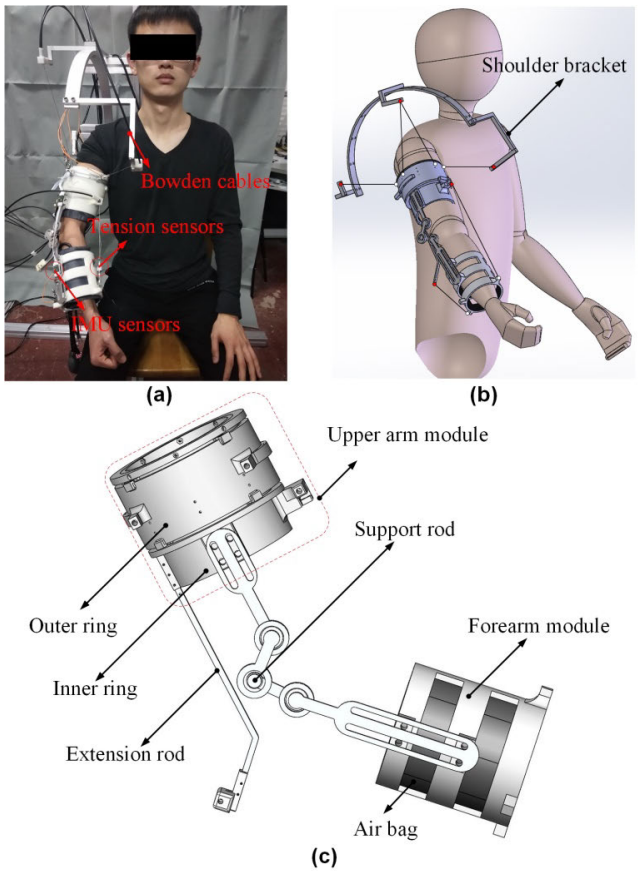

FIGURE 3. (a) The prototype of this robot worn by the user; (b) the 3D model of this robot; (c) the 3D model of the components worn on the arm.

This paper proposed the DAS to eliminate the singularities of the internal/external rotation DOF and improve the overall workspace and tension efficiency.

As shown in Figure 3, the upper arm module is made of nylon material by 3D printing. It is divided into two parts: the inner and outer rings. There are four cable attachment points on the outer ring and the shoulder bracket, respectively. The outer ring and the inner ring control the positive and negative rotation through a closed-loop cable. The two ends of this cable are connected to one motor of the drive system through two holes in the outer ring and through the Bowden cable. There are some small bearings between the inner and outer rings to ensure stable rotation. The rotation between the inner and outer rings is driven by one motor based on position mode. The distribution of the CAPs can be adjusted by the DAS in real-time. At the same time, the support rod is used to ensure the support of the patient's shoulder joint internal/external rotation, when his/her muscle strength is pretty weak, and the support rod does not limit the center position of the elbow joint and the length of the limb. The design description has also been presented in previous work [21].

As shown in Figure 4, during training, the DAS has two modes:

1) Compensation mode: when the current distribution of the CAPs cannot provide enough force/torque under the tension control strategy, the rotation changes the relative distribution of the CAPs to meet the strategy. Through the change of the CAPs distribution during the movement, combined with the initial CAPs optimization, the ADLs workspace can be realized almost 100% (the analysis is shown in the next section).

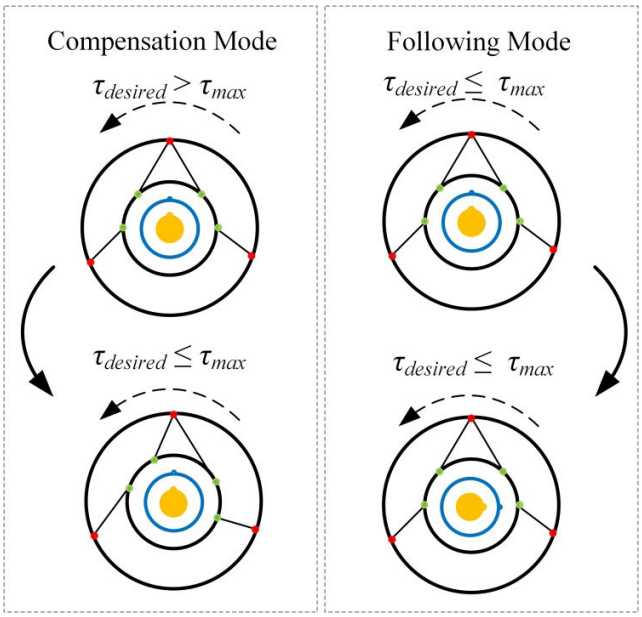

FIGURE 4. The large black circle, small black circle and blue circle represent the shoulder bracket, outer ring and inner ring of the upper arm module, respectively. The yellow circle represents the upper arm. The blue and yellow raised dots are used to visually show the direction of the relative rotation. The dashed arrow indicates the direction of torque.

2) Following mode: by increasing the DAS, the internal/external rotation of the shoulder joint can be independent of the flexion/extension and abduction/adduction, reducing the coupling between the joint motions so that the four cables will not interfere with the arm or the cables themselves even under a wide range of motion (such as external/internal rotation 90°). In the rotation movement, the CAPs on the upper arm module rotate in real-time, which can ensure a wide range of rotation motion without changing the configuration of the cables between the shoulder and upper arm modules. The singularity of the internal/external rotation DOF is eliminated. It is critical for increasing the robot's workspace.

At the same time, it should be noted that even if the DAS is added, the assistance and control of the internal and external rotation DOF are realized by four cables. The DAS is only used for the dynamic adaptation of CAPs. The overall control strategy is similar to the system without DAS, and this is also analyzed in Section IV.

B. MR-DASA DRIVE SYSTEM DESIGN

As mentioned in Section I, because the application of traditional electromechanical actuators introduces high intrinsic inertia, the compliant element (cables or Bowden cables) between the actuators and the output component of the robot lowers the natural frequency of the system, thus limiting its

dynamic performance. Compared to the conventional motor, the use of an MR clutch can weaken this effect since its low output inertia. Therefore, the MR is used for this cable-driven robot, which can improve the force-feedback performance and is very suitable for human-robot interaction, including the rehabilitation robot [19].

MR is a passive actuator, which outputs different damping according to different input currents. In order to actively generate and control the cable tension, the DASA drive system is needed, which consists of one power source and several MRs. In the proposed drive system, a high-ratio gear motor is selected as the power source. As shown in Figure 5 (b), the power motor rotates to drive the rotation of MRs in slippage, and a variable amount of torque is transmitted from the motor to the pulleys by modulating the amount of current that is supplied to the MR clutches. The MR pulls the cable through the cable reel [20]. In this design, in order to achieve modularity, the DASA drive system for elbow and shoulder training is independent. The elbow joint drive system is driven by only one power motor and two MRs. The shoulder joint system is more complicated, which consists of one power motor, four MRs, and one Z-axis motor for DAS. Therefore, this paper only demonstrates the drive system for the shoulder joint module. Figure 5 (a) shows the DASA system for the shoulder joint. Four MRs control the four cables of the shoulder joint, respectively, and the Z-axis motor is used to control the DAS. The performance of the drive system is demonstrated in Table 2.

TABLE 2. Performance of the drive system.

Parameter	Value
MR Maximal Torque	1.2 Nm
MR Maximal Current	1 A
MR Outer Diameter	42 mm
MR Width	38 mm
Power Motor Max Speed	700 rpm
Power Motor Max Torque	4 Nm
Z-axis Motor Max Speed	180 rpm
Z-axis Motor Max Power	48 W

III. ANALYSIS OF THE WORKSPACE AND TENSION EFFICIENCY

The last section has proposed the method for increasing workspace and the mechanical design of the DAS. In this section, the optimization of the initial distribution of the CAPs and the analysis of the workspace and cable tension efficiency are presented.

The assumptions of parameters about the optimization of CAPs have been shown in the previous work [21]. The length of the limb is set as $l_u = 320\ mm$, $l_{um} = 200\ mm$, $l_f = 250\ mm$, and $l_{fm} = 180\ mm$. Therein, l_u is from the shoulder joint center to the elbow joint center, l_{um} is from the shoulder joint center to the upper arm module center, l_f is from the elbow joint center to the wrist joint center, and l_{fm} is from the elbow joint center to the forearm module center. To avoid the interference between the human limb and the exoskeleton, the radius of the shoulder bracket, the upper arm ring and the forearm ring are *250 mm*, *120 mm,* and *110 mm*, respectively. In order to avoid interference between the cables and the limbs, in the compensation mode, the relative rotation angle of the inner and outer rings is limited to *35°*. So, what needs to be optimized is the initial distribution of CAPs.

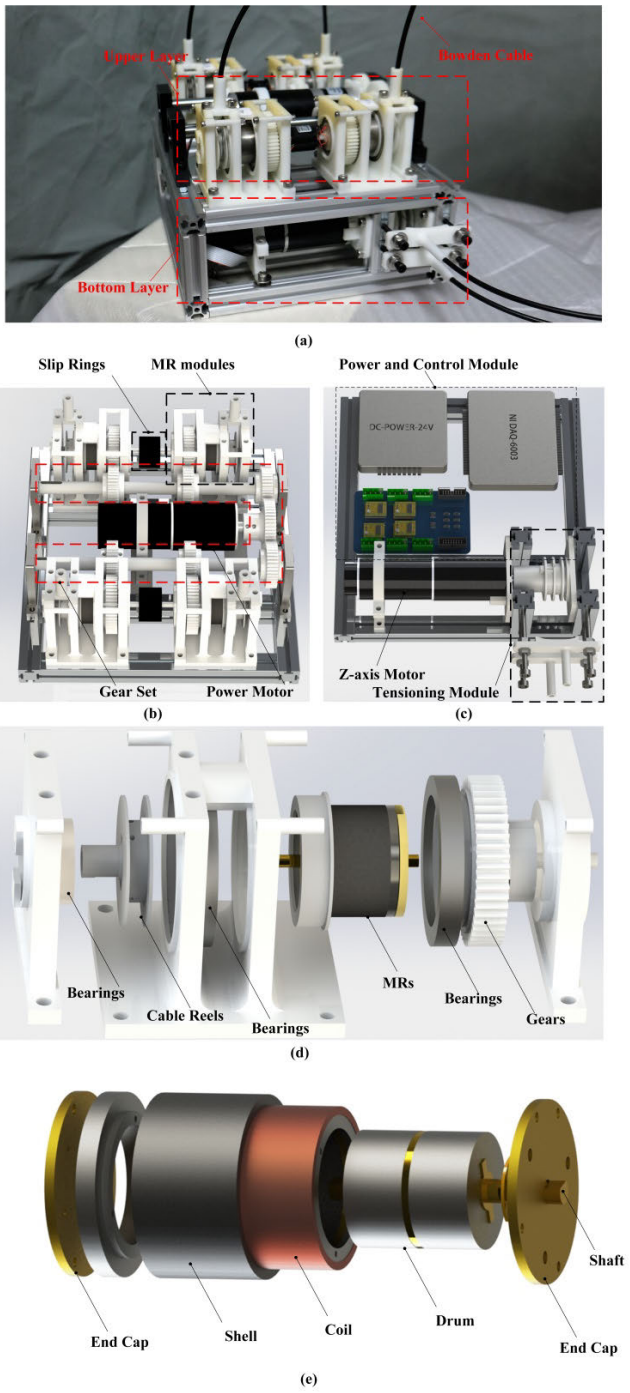

FIGURE 5. The drive system: (a) the prototype of the drive system, (b) the upper layer, (c) the bottom layer, (d) the exploded view of the MR-Cable unit, (e) the MR clutch assembly.

The optimization process is shown in Figure 6. The optimization target space is set as ADLs space, and the whole space is divided into *12360* points. Each point is

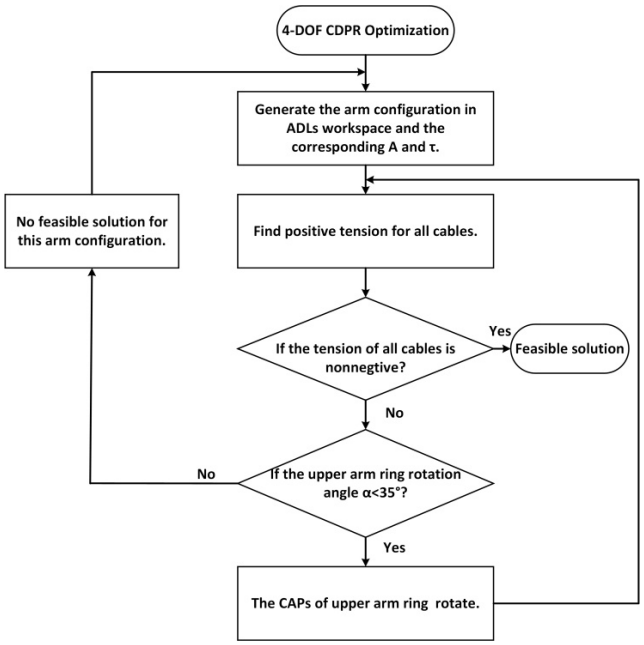

FIGURE 6. The optimization process of the workspace.

calculated according to the *eq. (2) -(7)* in Section IV to determine whether it is feasible. The final result is shown in Figure 7. However, considering that the range of the elbow joint is mechanically limited, the final workspace is shown in Table 1.

In the compensation mode, the maximum output torque can be further increased to provide desired torque to some extent. In the following mode, the movement of the internal/external rotation DOF will not change the configuration of the cables, which is different from the other cable-driven exoskeletons. These two modes can greatly improve the overall workspace. Figure 7 shows the difference in the workspace with/without DAS. The three-dimensional diagram cannot fully describe the feasible workspace of the 4-DOF robot, but it is also sufficient to show the significant improvement.

Figure 8 shows the optimized CAPs distribution of the proposed robot *(C1)* and a conventional cable-driven robot without DAS *(C2)*. By comparing the difference of the tension efficiency and workspace between these two robots, it can be shown that the great contribution of the DAS to the system performance. Although the addition of DAS is equivalent to the addition of one cable, it is impossible to achieve the performance of the proposed robot if a conventional cable-driven structure with five cables is adopted.

The difference of the workspace can be easily found from the joint angle range in TABLE 3. For comparison of the tension efficiency, the average tension efficiency is defined by when the maximum tension of each cable is set to *85 N*, in the whole workspace, the average of maximum torque in the positive and negative direction of each DOF.

Obviously, the robot proposed in this paper has great advantages in the workspace and cable tension efficiency. When the workspace is limited to a small one, like the

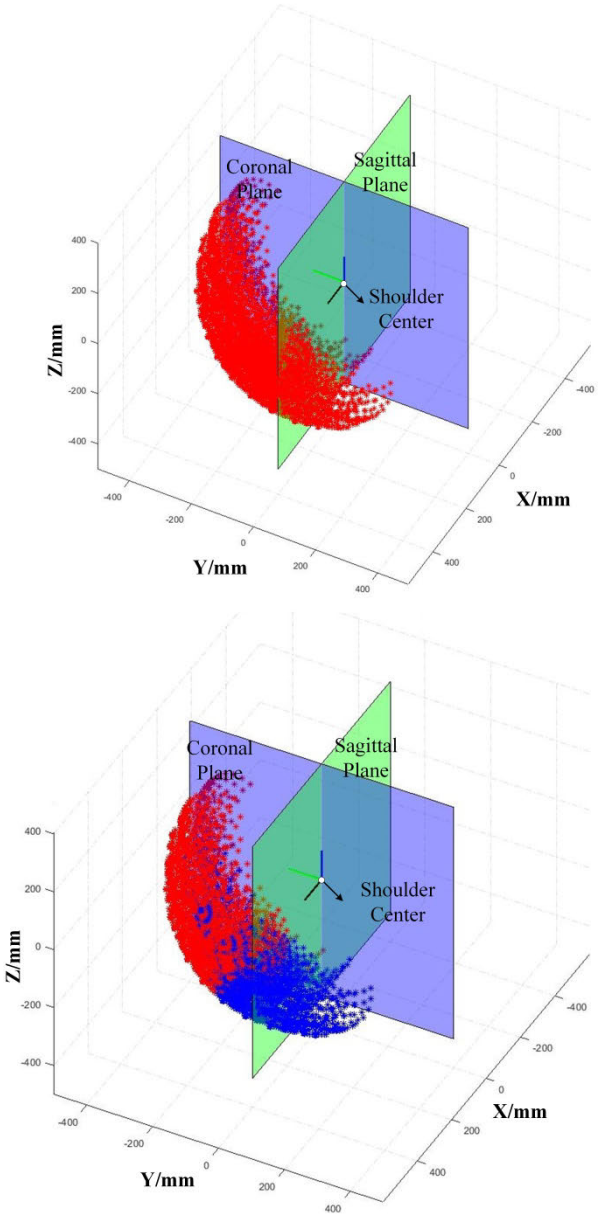

FIGURE 7. The optimized workspace, where blue points are infeasible and red points are feasible: (a) with DAS, (b) without DAS.

workspace of *C2*, the advantages are more obvious, and there is no potential uncontrollability. It is abnormal in the *X* because the optimized configuration is anisotropic, and the maximum torque that can be generated in each direction is different, but it does not exceed the proposed robot much. The proposed robot has great overall performance in both workspace and tension efficiency.

IV. CONTROL ALGORITHM

A. DYNAMIC ANALYSIS

The dynamic modeling for this 4-DOF robot is presented as follows:

$$D(q)\ddot{q} + C(q,\dot{q})\dot{q} + g(q) = J(q)^T T(t) \tag{1}$$

where D denotes the inertia matrix, C denotes Coriolis and centrifugal term, and G denotes the gravity term of both device and the human limb, q represents the joint angular, and $J(q)$ is the Jacobian matrix relating cable tensions to joint moments, and $T(t)$ is the vector of cable tensions. Due to the characteristic of cables, the tension must be kept positive for system control. The tension planner can be expressed as:

$$AT = \tau \tag{2}$$

where $A = J(q)^T$ in (1), τ is the torque that is required at the joints to drive the arm. Because the number of cables is more than the number of DOFs, the solution of (2) can be written as:

$$T = \bar{T} + N(A)m \tag{3}$$

where T is the minimum norm solution of (2) which is given by:

$$\bar{T} = A^T(AA^T)^{-1}\tau \tag{4}$$

$N(A)$ is a null space matrix of A and m is a 2×1 vector of arbitrary, assuming A is full rank. Considering the constraints of tensions, the planner can be expressed as:

$$\begin{bmatrix} N(A) \\ -N(A) \end{bmatrix} m \geq \begin{bmatrix} T_{\min} - \bar{T} \\ -T_{\max} + \bar{T} \end{bmatrix} \tag{5}$$

Finally, the optimal solution of cable tensions can be found as the following:

$$\min \sum_i (\bar{T} + N(A)m)_i \tag{6}$$

$$s.t.\ \ T_{\min} \leq T + N(A)m \leq T_{\max} \tag{7}$$

T_{max} is the upper bound of tension, which is set as $85\ N$ in this paper, and T_{min} is the lower bound, which is $2\ N$.

B. MR-CABLE TENSION CONTROL ALGORITHM

In order to reduce the influence of friction, this paper chooses a *1 * 7* multi-strand steel cable with a diameter of 1mm. Both the cable shell and the Bowden cable inner sleeve are made of PTFE material to minimize viscous friction. The Bowden cable inner sleeve is selected from the longitudinal construction of flat-band steel to reduce the effect of its elasticity on the system. The diameter of the Bowden cable is *5 mm*. In the meantime, according to the model proposed in [22], the feedforward compensation of the friction is achieved. A closed-loop tension control model was established to compensate for the effects of the unmodeled friction and MR hysteresis. The control block diagram is shown in Figure 9. The tension controller calculates the MR clutch input command according to the friction compensation model and the PI controller. The MR clutch adjusts the output torque according to the command, which is converted into cable tension through the reel, and the encoder detects the cable movement direction.

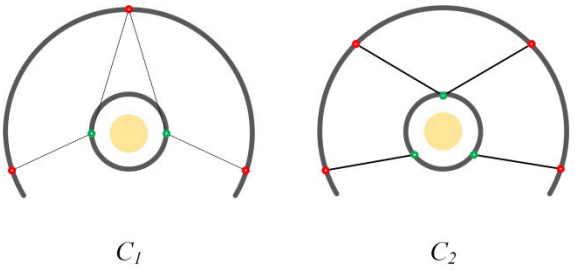

FIGURE 8. The optimized CAPs distribution of the proposed robot (C1) and a conventional robot without DAS (C2).

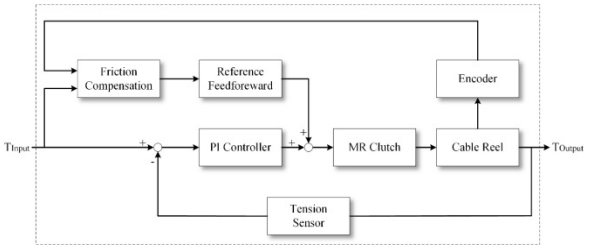

FIGURE 9. The MR-Cable tension control block diagram.

C. PASSIVE AND ACTIVE TRAINING CONTROL ALGORITHM

With the DAS, the cable-driven robot is still controlled based on cable tension. The controller is divided into high-level and low-level controllers. The high-level controller is used to calculate the desired 3-axis torque according to the training mode and decompose the torque to the tension of each cable according to *(1) - (7)*. The low-level controller is used to keep the cable tensions as the calculation value of the tension planner.

For passive training, the PID controller is used to drive the limb to move along the set trajectory:

$$-J(q)^T T(t) = K_D\dot{e} + K_P e + K_I \int_0^t e(s)ds + G_0(q) \tag{8}$$

where $e = q_d - q$, q_d is the desired joint angle, q is the actual joint angle. $G_0(q)$ is the initial gravity vector to compensate the weight, $K_D = 100I$, $K_P = 300I$, *and* $K_I = 25I$ are the derivative, proportional and integral gains of the controller, respectively.

For active training, the impedance controller is applied to provide proper assistance, and the controller can be written:

$$-J(q)^T T(t) = G(q) + K_r e - B_r\dot{q} \tag{9}$$

where K_r and B_r are, respectively, the stiffness and damping, and they can be adjusted to provide different assistance according to the patient recovery condition. The control diagram overview is shown in Figure 10. The proposed controller consists of the high-level tension planner and the low-level cable tension controller. But in the tension planner, the controller of the DAS is added. The DAS is controller based on position and follows the arm internal/external rotation in the following mode. In the compensation mode,

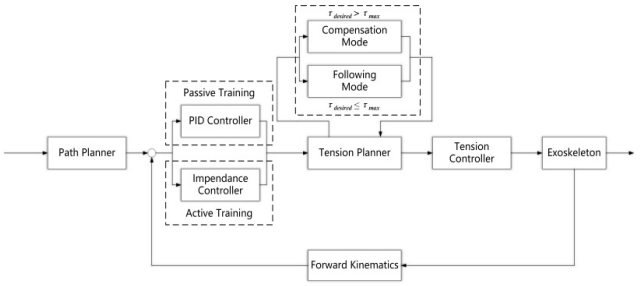

FIGURE 10. The system control block diagram.

it rotates to increase the effective torque. The control command of the DAS is given by the tension planner.

V. EXPERIMENT AND ANALYSIS

A. MR PERFORMANCE EXPERIMENT

To demonstrate the performance of the MR clutches and MR-Cable system, the following sets of experiments were carried out. The MR performance test platform is shown in Figure 11 (a). The motor drives the MR clutch to rotate by the coupling, and the force gauge at the end of the linkage measures and records the output of MR at a given current and the step response. The MR-Cable system test platform is presented in Figure 11 (b), the end of the one cable is connected to the fixed base, and the tension is measured and recorded by the tension sensor.

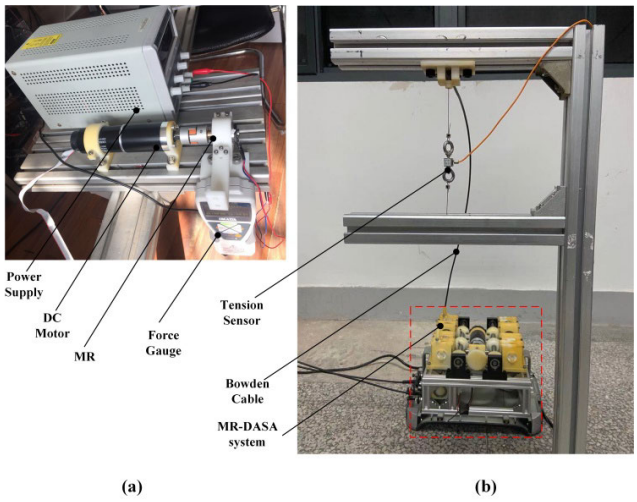

FIGURE 11. The system performance test platform: (a) the MR clutch test platform, (b) the MR-Cable system test platform.

Figure 12 (a) shows the MR current-torque curve. It can be seen that there is a certain hysteresis between the ramp up and down. Figure 12 (b) shows the MR step response curve. It can be seen that the MR clutch has a high step response speed. Combined with the low output inertia of the MR clutch, the MR-Cable system has a high dynamic performance. As shown in Figure 12 (c), for the MR-Cable closed-loop force control Bode diagram, the input was a sinusoidal signal with amplitude 30 N, the frequency growth

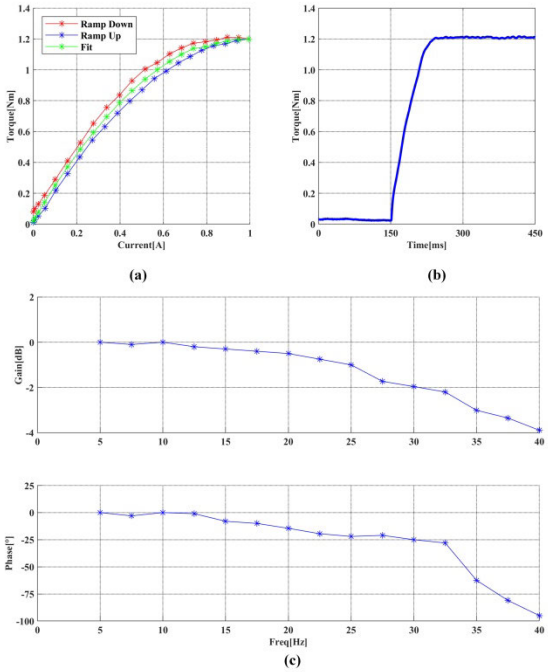

FIGURE 12. The performance of the MR clutches and MR-Cable system: (a) the MR current-torque curve, (b) the MR step response curve, (c) the MR-Cable closed-loop force control Bode diagram.

TABLE 3. The workspace and tension efficiency comparison.

	Workspace			Average Tension Efficiency / Nm		
	q_1	q_2	q_3	X(q_1)	Y(q_2)	Z(q_3)
C1	[-25+80]	[-120,+25]	[-90,+90]	6.693	7.347	5.867
C2	[-25,+80]	[-50, +10]	[-20,+20]	9.589	5.8755	3.519
C1_2	[-25,+80]	[-50, +10]	[-20,+20]	9.572	8.876	6.955

Note: The *C1_2* represents the average tension efficiency in the whole workspace of *C2*, but the distribution of the CAPs is *C1*. q_1, q_2 and q_3 have been defined in Table I.

step is 2.5 Hz, the gain and phase of each point were recorded. The bandwidth of this system is about 35 Hz at −3 dB and is fully superior to the human force bandwidth that is between 5 and 10 Hz [23].

Figure 13 shows a set of cable tension tracking curves collected in the experiment. With the conventional motor drive system (MAXON RE40), the maximum error is *3.55 N*, and the root mean square error (RMSE) is *0.88 N*. With the proposed MR-DASA drive system, the maximum error is *1.35 N*, and the RMSE is *0.38 N*. It can be seen that the cable tension tracking is more accurate and stable with MR-DASA drive system, and the overshoot phenomenon is significantly reduced.

B. PASSIVE TRAINING WORKSPACE VERIFICATION EXPERIMENT

The passive training experiment is conducted to verify the adaption of this exoskeleton, the passive control algorithm,

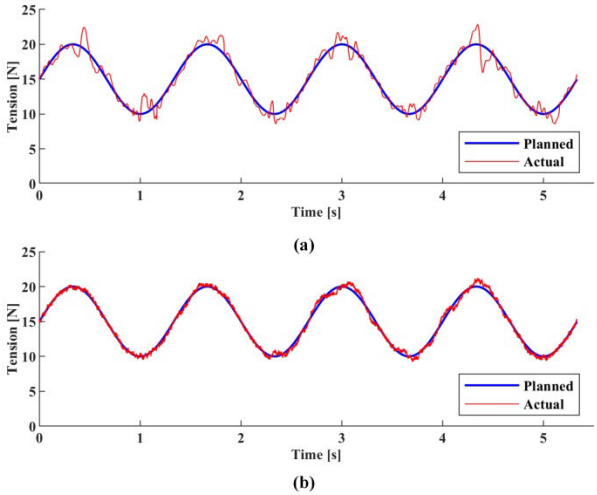

FIGURE 13. The cable tension tracking experiment: (a) with the conventional motor drive system, (b) with the MR-DASA drive system.

TABLE 4. The body parameters of three subjects.

ID	Weight/kg	Height/cm	l_u/cm	l_{um}/cm	l_f/cm	l_{fm}/cm
S1	65	182	30.1	20	25.9	18
S2	55	172	27.9	20	24.6	18
S3	58	161	26.4	19	21.1	17

and the function of the DAS. This experiment has been conducted in the previous research, and the exoskeleton was driven by the electric motors [21]. As shown in Table 4, three healthy subjects with different body sizes were selected in the experiment. The trajectory was set as: firstly, the abduction and flexion of the shoulder joint from $0°$ to $60°$, simultaneously; then, the flexion of the elbow joint from $0°$ to $60°$; finally, the internal rotation of the shoulder joint from $0°$ to $30°$. After several seconds, the arm was driven to the initial posture, following the reverse trajectory. The above is one complete movement, and each subject repeated the complete movement five times.

In Figure 14, as shown by the green curve, it is the angle of the rotation structure. During P1, since the moment at the rotation direction generated by the arm weight cannot be balanced with the distribution of cable attachment points, the DAS worked in compensation mode. During P2, the DAS worked in the following mode. It is possible to complete the arm rotation without the change of the distribution of the cable attachment points. After the elbow joint restores to the initial condition, the DAS also restores to the initial condition and waits for the next response.

The workspace experiment was carried out to verify the effective workspace. The subjects relaxed their limbs, and the robot worked in passive mode. The limb was driven by the robot to move in the maximum angle range of each joint. In the experiment, all three subjects can reach the theoretical maximum angle shown in Table 1. The key posture of S1 is shown in Figure 15. The bending angle of Bowden cables for tension control is small to increase the tension efficiency,

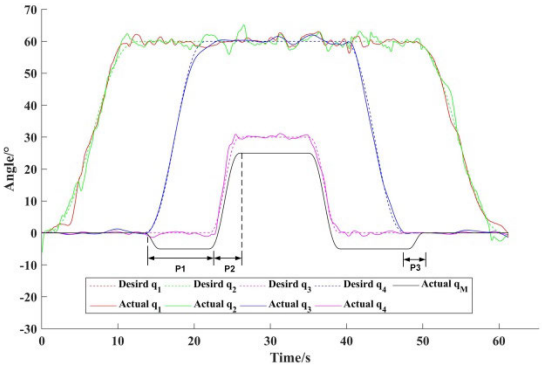

FIGURE 14. The actual trajectory and desired trajectory during one complete movement of the experiments of the subject S1: P1 is the flexion movement of the elbow joint; P2 is the internal rotation movement of the shoulder joint; P3 is the waiting period.

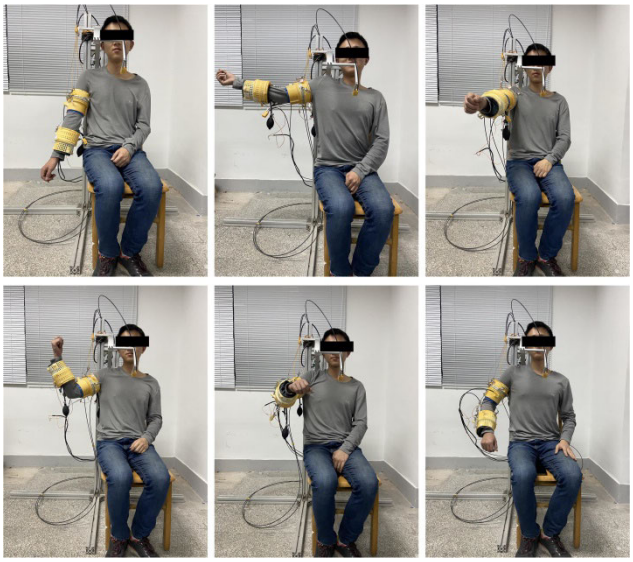

FIGURE 15. The key posture of S1 in the workspace experiment.

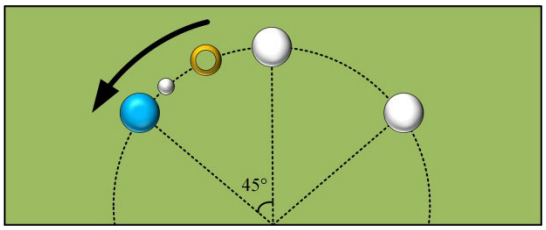

FIGURE 16. Active training virtual game, the blue dot is the current target point, the small white dot is the guide point, and the yellow ring represents the current position.

and the significantly bent Bowden cables are used for rotation angle control of DAS.

C. ACTIVE TRAINING EXPERIMENT

The active training experiment was carried out to verify the response performance of the following mode. As shown in Figure 16, the virtual scene is designed to guide the subjects' movement. The subject wore the exoskeleton and

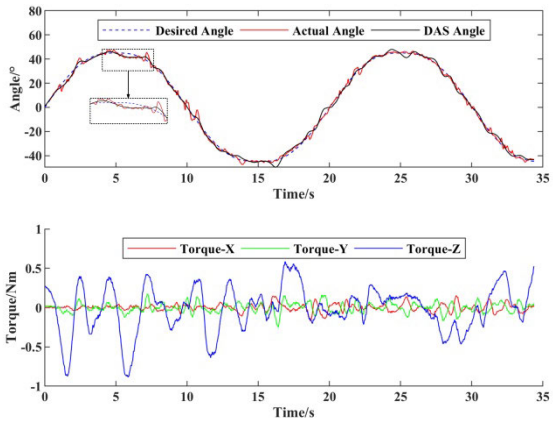

FIGURE 17. The angle and torque during active training.

controlled the yellow ring to follow the small white dot until it reaches the target blue dot. During the training, the robot worked in the active training mode and provided the proper assistance for the subject. Only the internal/external rotation was provided the force-feedback according to the impedance control algorithm, and the other two DOFs are kept in a comfortable position. The DAS works in the following mode.

The experiment results are demonstrated in Figure 17. The DAS can follow the limb at the joint velocity 0.16 rad/s. In the following mode, the DAS can follow the rotation of the limb, keep the configuration of the cables and provide a large feasible workspace and high tension efficiency. The overall performance in the following mode was good, and the robot can provide force feedback to help them complete the movement better. There was a certain moment coupling in the other two DOFs, which was caused by the IMU measurement error and a certain cable tension error.

VI. DISCUSSION AND CONCLUSION

In order to improve the workspace, tension efficiency, and force bandwidth of cable-driven exoskeletons for shoulder-elbow rehabilitation, this paper analyzes the core reasons by simplifying the model and proposed an optimized structure design. Unlike the traditional CAPs distribution optimization, this paper proposed the DAS to make the CAPs distribution dynamically change. Therefore, the singularity of internal/external rotation DOF is eliminated, and the overall workspace and cable efficiency of all three DOFs are increased. The DAS can work in compensation or following mode to provide enough torque, keep high cable tension efficiency and avoid interference between the limb and cables. Besides, in order to reduce the effects of compliant elements between the actuators and output and to improve the force bandwidth, we designed the DASA drive system composed of the geared DC motor and MR clutches. A control algorithm for this robot system was designed for tension control and active and passive rehabilitation training.

In order to verify the performance of the system, several experiments were designed. In the drive system performance test experiment, it can be obtained that the bandwidth of the MR-DASA cable-driven system is about 35Hz, which is fully superior to the human force bandwidth. Through the cable tension tracking experiment, it can be found that the cable tension control performance of the proposed drive system is significantly better than that of the traditional actuators, which improves the force feedback performance of rehabilitation training. A passive training experiment verifies the function of the DAS, and the results show that the DAS can work well in two modes. However, due to some uncertain parameters in the system, such as shoulder joint center shift and limb length measurement errors, there are certain errors in position control. In future work, the identification of uncertain parameters can be achieved through model and calculation according to cable length, thereby improving accuracy. The experimental results of the workspace show that the exoskeleton system can achieve ADLs workspace for subjects of different sizes. However, in the clinical rehabilitation training, because the parasitic force cannot be completely eliminated and it is related to the actual torque provided if the patient is in a state of high muscle tension, it is not recommended to use this system. In order to further verify the tracking performance of the DAS, an active training experiment was designed. In the experiment, the DAS always worked in the following mode to ensure the cable tension efficiency and avoid singularities. The results show that the DAS can track the subject's arm motion well at least at a speed of 0.16 rad/s.

In summary, the proposed exoskeleton greatly improves the workspace and cable tension efficiency by adding the DAS. With the MR-DASA system, the tension control performance is also improved. Compared with existing cable-driven exoskeletons, like CAREX, the exoskeleton proposed in this paper does not increase the system complexity too much. The whole system is still very compact and lightweight. The upper arm and forearm module radii are smaller than CAREX, and the wearable weight is also lighter than it. It is important that this exoskeleton achieves the coverage of the ADLs space and eliminates the potential danger caused by exceeding the workspace. In the meantime, the cable tension efficiency is higher, the parasitic force is smaller, which improves the comfort and safety of rehabilitation training. The cable tension control performance is better, and it can provide better torque output in active and passive training.

In future work, the AAN training algorithm based on the cable-driven exoskeleton will be developed and optimized. And the clinical trials will be conducted under the guidance of professional therapists to verify the rehabilitation effectiveness for post-stroke patients.

ETHICAL STATEMENT

All procedures performed in studies involving human participants were in accordance with the ethical standards of the institutional and/or national research committee and with the 1964 Helsinki declaration and its later amendments or comparable ethical standards. And this study is approved by the ethics committee of Jiangsu Province Hospital. Informed and

written consent was obtained from all individual participants included in the study.

CONFLICT OF INTEREST

The authors declare that the research was conducted in the absence of any commercial or financial relationships that could be construed as a potential conflict of interest.

REFERENCES

[1] P. S. Lum, C. G. Burgar, P. C. Shor, M. Majmundar, and M. Van der Loos, "Robot-assisted movement training compared with conventional therapy techniques for the rehabilitation of upper-limb motor function after stroke," *Arch. Phys. Med. Rehabil.*, vol. 83, no. 7, pp. 952–959, Jul. 2002.

[2] Y. Ren, S. Hoon Kang, H.-S. Park, Y.-N. Wu, and L.-Q. Zhang, "Developing a multi-joint upper limb exoskeleton robot for diagnosis, therapy, and outcome evaluation in neurorehabilitation," *IEEE Trans. Neural Syst. Rehabil. Eng.*, vol. 21, no. 3, pp. 490–499, May 2013.

[3] J. C. Perry, J. Rosen, and S. Burns, "Upper-limb powered exoskeleton design," *IEEE/ASME Trans. Mechatronics*, vol. 12, no. 4, pp. 408–417, Aug. 2007.

[4] A. Alamdari and V. Krovi, "Modeling and control of a novel home-based cable-driven parallel platform robot: PACER," in *Proc. IEEE/RSJ Int. Conf. Intell. Robots Syst. (IROS)*, Sep. 2015, pp. 6330–6335.

[5] J. F. Veneman, R. Ekkelenkamp, R. Kruidhof, F. C. T. van der Helm, and H. van der Kooij, "Design of a series elastic and bowden cable-based actuation system for use as torque-actuator in exoskeleton-type training robots," in *Proc. IEEE Int. Conf. Rehab. Robot. (ICORR)*, Oct. 2005, pp. 496–499.

[6] Y. Mao and S. K. Agrawal, "Design of a cable-driven arm exoskeleton (CAREX) for neural rehabilitation," *IEEE Trans. Robot.*, vol. 28, no. 4, pp. 922–931, Aug. 2012.

[7] S. K. Mustafa, G. Yang, S. H. Yeo, and W. Lin, "Optimal design of a bio-inspired anthropocentric shoulder rehabilitator," *Appl. Bionics Biomech.*, vol. 3, no. 3, pp. 199–208, Jan. 2006.

[8] B. Zi, B. Wang, and D. Wang, "Design and analysis of a novel cable-actuated palletizing robot," *Int. J. Adv. Robot. Syst.*, vol. 14, no. 6, Nov. 2017, Art. no. 172988141774108.

[9] G. Yang, S. K. Mustafa, S. H. Yeo, W. Lin, and W. B. Lim, "Kinematic design of an anthropomimetic 7-DOF cable-driven robotic arm," *Frontiers Mech. Eng. China*, vol. 4, pp. 45–60, Dec. 2010.

[10] S. K. Mustafa and S. K. Agrawal, "On the force-closure analysis of n-DOF cable-driven open chains based on reciprocal screw theory," *IEEE Trans. Robot.*, vol. 28, no. 1, pp. 22–31, Feb. 2012.

[11] R. M. Murray, Z. Li, and S. S. Sastry, *A Mathematical Introduction to Robotic Manipulation*. Boca Raton, FL, USA: CRC Press, 1994, pp. 1–456.

[12] Y. Mao, X. Jin, and S. K. Agrawal, "Real-time estimation of glenohumeral joint rotation center with cable-driven arm exoskeleton (CAREX)—A cable-based arm exoskeleton," *J. Mech. Robot.*, vol. 6, no. 1, Feb. 2014.

[13] S. Kurbanhusen Mustafa, G. Yang, S. Huat Yeo, W. Lin, and I.-M. Chen, "Self-calibration of a biologically inspired 7 DOF cable-driven robotic arm," *IEEE/ASME Trans. Mechatronics*, vol. 13, no. 1, pp. 66–75, Feb. 2008.

[14] Z. Li, W. Chen, J. Zhang, and S. Bai, "Design and control of a 4-DOF cable-driven arm rehabilitation robot (CARR-4)," in *Proc. IEEE Int. Conf. Cybern. Intell. Syst. (CIS) IEEE Conf. Robot., Autom. Mechatronics (RAM)*, Nov. 2017, pp. 581–586.

[15] Z.-F. Shao, X. Tang, and W. Yi, "Optimal design of a 3-DOF cable-driven upper arm exoskeleton," *Adv. Mech. Eng.*, vol. 6, Jan. 2014, Art. no. 157096.

[16] I. Galiana, F. L. Hammond, R. D. Howe, and M. B. Popovic, "Wearable soft robotic device for post-stroke shoulder rehabilitation: Identifying misalignments," in *Proc. IEEE/RSJ Int. Conf. Intell. Robots Syst. (IROS)*, Oct. 2012, pp. 317–322.

[17] I. Gaponov, D. Popov, S. J. Lee, and J.-H. Ryu, "Auxilio: A portable cable-driven exosuit for upper extremity assistance," *Int. J. Control, Autom. Syst.*, vol. 15, no. 1, pp. 73–84, Feb. 2017.

[18] X. Cui, W. Chen, X. Jin, and S. K. Agrawal, "Design of a 7-DOF cable-driven arm exoskeleton (CAREX-7) and a controller for dexterous motion training or assistance," *IEEE/ASME Trans. Mechatronics*, vol. 22, no. 1, pp. 161–172, Feb. 2017.

[19] J. Viau, P. Chouinard, J.-P.-L. Bigue, G. Julio, F. Michaud, and J.-S. Plante, "Tendon-driven manipulator actuated by magnetorheological clutches exhibiting both high-power and soft motion capabilities," *IEEE/ASME Trans. Mechatronics*, vol. 22, no. 1, pp. 561–571, Feb. 2017.

[20] K. Shi, A. Song, Y. Li, H. Li, D. Chen, and L. Zhu, "A cable-driven three-DOF wrist rehabilitation exoskeleton with improved performance," *Frontiers Neurorobot.*, vol. 15, Apr. 2021, doi: 10.3389/fnbot.2021.664062.

[21] K. Shi, A. Song, Y. Li, D. Chen, and H. Li, "Cable-driven 4-DOF upper limb rehabilitation robot," in *Proc. IEEE/RSJ Int. Conf. Intell. Robots Syst. (IROS)*, Nov. 2019, pp. 6465–6472.

[22] G. Palli and C. Melchiorri, "Model and control of tendon-sheath transmission systems," in *Proc. IEEE Int. Conf. Robot. Autom.*, 2006, pp. 988–993.

[23] K. B. Shimoga, "Finger force and touch feedback issues in dexterous telemanipulation," in *Proc. 4th Annu. Conf. Intell. Robot. Syst. Space Explor.*, 1992, pp. 159–178.

KE SHI received the B.S. degree from the School of Instrument Science and Engineering, Southeast University, Nanjing, China, in 2016, where he is currently pursuing the Ph.D. degree. His current research interests include rehabilitation robotics and human–robotic interaction.

AIGUO SONG (Senior Member, IEEE) was born in Huangshan, China, in 1968. He received the B.S. degree in automatic control and the M.S. degree in measurement and control from the Nanjing University of Aeronautics and Astronautics, Nanjing, China, in 1990 and 1993, respectively, and the Ph.D. degree in measurement and control from Southeast University, Nanjing, China, in 1996.

From 1996 to 1998, he was an Associate Researcher with the Intelligent Information Processing Laboratory, Southeast University. From 1998 to 2000, he was an Associate Professor with the Department of Instrument Science and Engineering, Southeast University. From 2000 to 2003, he was the Director of the Robot Sensor and Control Laboratory, Southeast University. From April 2003 to April 2004, he was a Visiting Scientist with the Laboratory for Intelligent Mechanical Systems, Northwestern University, Evanston, IL, USA. He is currently a Professor with the School of Instrument Science and Engineering, Southeast University. His current research interests include concentrate on teleoperation, haptic display, Internet telerobotics, and distributed measurement systems.

HUIJUN LI received the B.S. degree in instrument science and the M.S. degree in condensed matter physics from Zhengzhou University, Zhengzhou, China, in 1999 and 2002, respectively, and the Ph.D. degree in measurement and control from Southeast University, Nanjing, China, in 2005.

She is currently an Associate professor with the Department of Instrument Science and Engineering. Her current research interests include teleoperation and rehabilitation robotics.